Contrib. Plasma Phys. **54**, No. 7, 626 – 634 (2014) / **DOI** 10.1002/ctpp.201300047

Particle in Cell/Monte Carlo Collision Method for Simulation of RF Glow Discharges: Effect of Super Particle Weighting

E. Erden and **I. Rafatov***

Middle East Technical University, Ankara, Turkey

Received 24 August 2013, revised 05 October 2013, accepted 13 October 2013
Published online 09 December 2013

Key words Glow discharge, particle-in-cell method, plasma simulations, Monte Carlo methods.

A parallel Particle in Cell/Monte Carlo Collision (PIC/MCC) numerical code for glow discharge plasma simulations is developed and verified. This method is based on simultaneous solution of the Lorentz equations of motion of super particles, coupled with the Poisson's equation for electric field. Collisions between the particles are modelled by the Monte Carlo method. Proper choice of particle weighting is critically important in order to perform adequate and efficient PIC simulations of plasma. Herein, effects of particle weighting on the simulations of capacitive radio-frequency argon plasma discharges are studied in details.

1 Introduction

Low pressure and temperature glow discharge plasmas have a wide variety of usage in the industrial applications such as surface activation of polymers, etching and deposition [1]. There are mainly three types of numerical simulation techniques to investigate the glow discharges: fluid (continuum), kinetic (particle) and hybrid methods [2].

Within the typical fluid model, continuity and momentum equations of charged particles, reduced to the drift-diffusion equations, are solved simultaneously with the Poisson's equation for electric field. Ionization source terms as well as diffusion and mobility coefficients are calculated as functions of local values of electric field [3,4]. In general, fluid models are self consistent and fast compared to kinetic models. However, they may not always describe plasma correctly. For some plasmas of interest, ratio of the mean free path of charged particles (mainly the electrons) to plasma dimensions may not be small enough to relax and obtain a Maxwellian distribution. Therefore different energy groups of particles can be created in the discharge, leading to loss of thermodynamic equilibrium [5]. In such cases, it is useful to apply the kinetic model, which may involve either direct solution of the kinetic Boltzmann equation or particle method. Finally, in a hybrid model, a combination of particle and fluid models, slow electrons and ions are treated as fluids, whereas fast electrons are described by the particle method, employing Monte Carlo method for collisions [6]. This method has speed advantage of fluid and accuracy of particle methods.

In present work, we developed and verified a parallel 1d3v Particle in Cell/Monte Carlo Collision (PIC/MCC) numerical code for the glow discharge plasma simulations. This method is based on the simultaneous solutions of the Lorentz equations of motion for super particles, coupled with the Poisson's equation for electric field. Collisions between the particles are modelled by the Monte Carlo method [7]. The issue of particle weighting is often ignored in particle studies, even though it can play a crucial role in developing an efficient and adequate simulation of plasma. In this paper, the effects of particle weighting on the PIC/MCC simulation results are investigated. More precisely, this study aims to clarify the question of an adequate number of super particles per grid cell, sufficient to obtain reliable weighting independent characteristics of plasma. For test simulations, various cases of capacitively coupled RF discharges sustained in argon and helium gases are studied.

The algorithm and acceleration methods (parallelization and subcycling), applied in the code, are described in section 2. In section 3, numerical code for the helium plasma is verified by comparing with the results of the

* Corresponding author. E-mail: rafatov@metu.edu.tr, Phone: +90 312 210 3254, Fax: +90 312 210 5099

benchmark study [8]. Effect of super particle weighting is investigated for the argon plasma in section 4. Finally, a short summary is given in section 5.

2 PIC/MCC model

Unlike continuum methods, PIC/MCC method deals with the charged super particles. Each super particle consist of predefined number of particles of the same type (i.e. electrons, Ar^+, He^+ ions etc.), and this number is called weighting (W) of the super particle. The algorithm of interest can be summarized as the following.

(i) *Initialization.* At first step, charged particles are distributed between the boundaries according to selected density profile. Uniform random distribution is one of the choices. Velocity components of the particles are specified using a Maxwellian distribution in Cartesian coordinate system as

$$v_s = \sqrt{-\ln(R_1) \times 2k_{\mathrm{B}}T/m} \times \sin(2\pi R_2), \tag{1}$$

where v_s is any of the three components (v_x, v_y, and v_z) [9]. Here k_{B}, T and m denote the Boltzmann constant, temperature and mass of the selected particle type respectively. Variables R_1 and R_2 refer to random numbers with uniform distribution between [0,1].

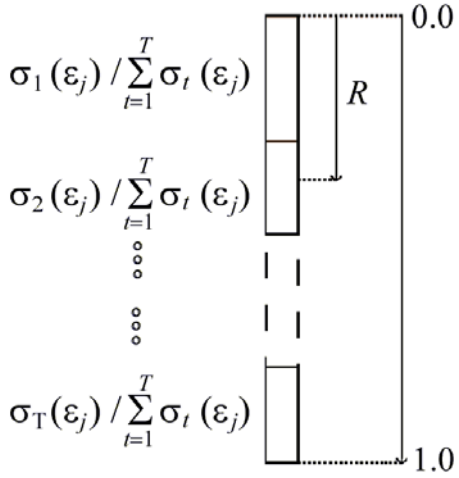

Fig. 1 Selection of the collision type for the j th particle, which can possibly do T types of collisions. Here σ_t is the cross section of the collision of type t, and ϵ_j is the energy of the j th particle.

(ii) *Calculation of charged particle densities on grid points.* Now that positions of super particles are known, one can find the particle densities on the grid points by using appropriate weighting method. In this study first order weighting is used [10]. In one-dimensional system, densities $n_{\mathrm{p}k}$ and $n_{\mathrm{p}k+1}$ of particles of type p on the two neighbour grid nodes k and $k+1$ are calculated using

$$n_{\mathrm{p}k} = W_{\mathrm{p}} \sum_{j=1}^{N} \frac{\Delta X_{j,\,k+1}}{\Delta x\, \Delta V}, \quad n_{\mathrm{p}k+1} = W_{\mathrm{p}} \sum_{j=1}^{N} \frac{\Delta X_{j,\,k}}{\Delta x\, \Delta V}, \tag{2}$$

where W_{p} is weighting of selected particle type, Δx is the size of the grid cell, $\Delta X_{j,\,k}$ and $\Delta X_{j,\,k+1}$ are the distances from the j th particle to the k and $k+1$ nodes, N is the number of super particles of type p locating between these nodes, $\Delta V = \Delta x \Delta y \Delta z$ is the volume element, where Δy and Δz are equal to one unit of length in the one-dimensional system.

(iii) *Solution of the Poisson's equation.* For a system with M types of charged plasma components, electric potential profile φ for the electrostatic plasmas of interest can be calculated by solving the Poisson's equation

$$\nabla^2 \varphi = -\frac{1}{\varepsilon_0} \sum_{\mathrm{p}=1}^{M} n_{\mathrm{p}} q_{\mathrm{p}}, \tag{3}$$

where ε_0 is the permittivity of free space, q_{p} is the charge of the particle of type p.

(iv) *Electric field calculation.* After obtaining the electric potential profile, electric field value E on grid points is obtained using equation

$$\mathbf{E} = -\nabla\varphi \tag{4}$$

with finite difference method. Fourth order central difference scheme for the inner nodes, forward and backward finite differences for the boundary nodes have been used in the simulations.

(v) *Interpolation of the electric field values to charged particles.* Electric field values on the grid points are interpolated to charged particles to determine forces acting on them.

(vi) *Solution of the Lorentz force equations, and implementation of the boundary conditions.* Equations

$$\frac{\mathrm{d}\mathbf{r}_j}{\mathrm{d}t} = \mathbf{v}_j, \tag{5}$$

$$\frac{\mathrm{d}\mathbf{v}_j}{\mathrm{d}t} = \frac{q_j}{m_j}\,\mathbf{E}_j \tag{6}$$

are solved to determine positions and velocity components of charged particles. Here q_j, m_j, $\mathbf{r}_j$, $\mathbf{v}_j$, and $\mathbf{E}_j$ denote the charge, mass, position and velocity of the jth particle, and the electric field acting on it. Explicit velocity-verlet algorithm is used to advance the particles to new positions and update the velocity components. The particles reaching the boundaries are identified and removed from the system if they don't reflect. Secondary electrons are added to the system if their emission is included in the model. Reflection and secondary electron emission processes are regulated by the Monte Carlo method.

(vii) *Collisions.* In the low pressure plasmas of interest, charged particle densities are at least $3-4$ orders of magnitude lower than that of the neutral background gas. Since the neutral–charged particle collisions dominate the collision processes, only electron-neutral and ion-neutral collisions are taken into account. Creation and interaction of metastables is relatively low at low pressure of interest [11], hence stepwise ionizations and metastables are not included in the simulations. Ion-neutral collisions are modeled with isotropic and backward (charge exchange) scattering approach [12]. Probability of a collision of the jth super particle over the time interval Δt is

$$P_j = 1 - \exp(-\nu_j\,\Delta t), \tag{7}$$

where ν_j denotes collision frequency. However doing the calculation for each super particles can be time consuming. Therefore, special algorithms such as null collision [13] can be applied to settle which particle will collide or not. After all the colliding particles are selected, types of collisions are identified by the Monte Carlo method according to the algorithm illustrated in Figure 1. It should be underlined that collision cross sections for ion-neutral collisions are calculated by using centre of mass energy [14]. After the collisions, new velocity components are assigned to collided particles, and the algorithm returns back to step (ii).

In order to have a good statistics, there should be a reasonably high number of particles per Debye length, $N_{\mathrm{D}} \gg 1$. Also, there are constraints while selecting space step Δx and time step Δt during the simulations: Δx must be of the order of the Debye length, and Δt should resolve oscillations of electrons, satisfy the Courant condition, and be sufficiently small to keep collision probability (7) reasonably small (for further details, see [7]). In general, for low pressure gas discharge simulations, the Courant condition

$$\Delta t < \Delta x / v_{\max} \tag{8}$$

is the most restrictive one. If it is not satisfied, particles may not move correctly and discontinuities in the total current profile may arise. To find the maximum possible speed $v_{\max}$, one can track the maximum velocity in the electron group in every time step, and set Δt accordingly. This is not an efficient approach, especially for the parallel codes. Maximum possible energy obtained by an electron during the simulations can be taken as absolute difference between the electrode potentials plus some arbitrary value (say 100 eV). The specified energy is converted to the maximum possible speed $v_{\max}$ for the electrons, which can be used to calculate the time step size Δt. This algorithm is more efficient and much easier to implement.

2.1 Parallelization of the algorithm

For each processing unit or worker the number of calculations per second is limited. It is reasonable to reduce the work/process done by each of them by parallelization to progress faster in time steps and consequently to reduce simulation times. There are mainly two types of parallelization schemes for PIC/MCC method: (1) Each of the processors/workers/CPUs are responsible from certain regions of the discharge; (2) All the workers are responsible from all of the grid nodes between the electrodes, but not from all the particles. In the latter case, super particle population is equally shared among the workers as much as possible. The first scheme has some disadvantages compared to the second one. These are

(i) The processors responsible from the border nodes are also assigned to manipulate the secondary electrons as well as to reflect the particles reaching the boundaries or remove them from the system. Therefore, there is a coding differentiation between the boundary and the inner workers, which makes coding more challenging.

(ii) Super particles are not static, they move over time. Consequently they may not stay assigned to the same CPU or location. In every time step of the simulations, particles may move from one grid point to another, i.e. from one worker to another. This situation creates extra communication, and one worker must be assigned to deal with the arrangements of the charged super particles between the processors.

(iii) If CPUs are responsible from equal number of grid points, then the CPUs responsible from quasi-neutral region of plasma deal with much more super particles than the ones accounted for the sheath regions. Hence the equal division of the work load may not be possible if this method is applied.

Our codes were developed according to the second scheme. With slight modifications, a standard single processor PIC/MCC code can be parallelized. Respectively, after the processors have calculated partial density profiles, these are sent to a predefined worker. (In our code processor #0 is assigned to this job, i.e. the master worker/processor). Master processor adds up all the density values coming from the other workers. Figure 2 illustrates the ion density profile contributed by one of the C workers and the overall ion density profile after the ion densities collected by the master worker. As the total density profile is computed by the master processor, the Poisson's equation can be solved,

$$\nabla^2\varphi = -\frac{1}{\varepsilon_0}\sum_{c=0}^{C-1}\left(\sum_{\mathrm{p}=1}^{M} n_{\mathrm{p}} q_{\mathrm{p}}\right)_c , \tag{9}$$

where C is the total number of processors. Master processor also calculates and broadcasts (CALL MPI_Bcast in MPI implementation of the fortran code) the electric field values. Processors only communicate at this part of the method. Summary of the parallel algorithm is shown in Figure 3.

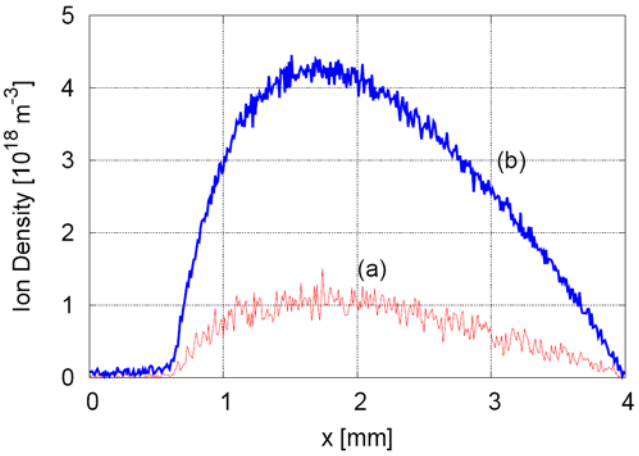

Fig. 2 Example of parallel PIC/MCC simulation: (a) ion densities accounted by the processor #1, (b) global sum of the ion densities computed by the master worker.

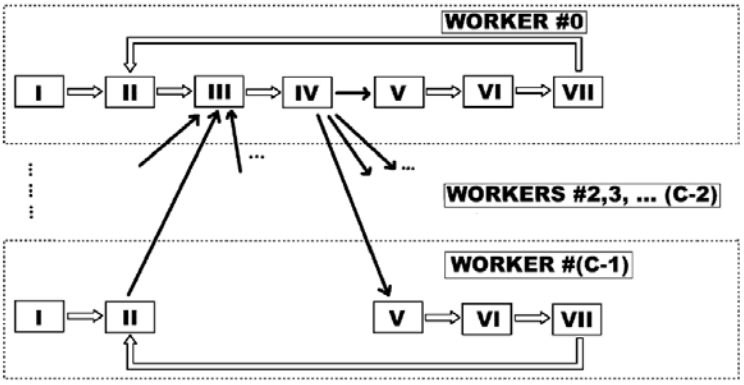

Fig. 3 Parallel PIC/MCC algorithm for a system with C processors. Black arrows refer to communications between the processors (MPI_Reduce & MPI_Bcast). Processor #0 is the master processor responsible for density collection, electric potential and electric field calculation and delivering these data to remaining workers. I) Initialization, II) Calculation of charged particle densities on grid points, III) Solution of the Poisson's equation, IV) Electric field calculation, V) Interpolation of electric field values to charged particles, VI) Solution of the Lorentz equations and implementation of boundary conditions, VII) Collisions.

2.2 Subcycling

In addition to the parallelization, subcycling of ions and slow electrons can be used to speed up the simulations [15]. Using this approach, ions and low energetic (slow) electrons are moved and collided not in every, but in $S_{\rm se}$'th (slow electron subcycling coefficient) and $S_{\rm i}$'th (ion subcycling coefficient) time steps. Within this method, high gains can be obtained in terms of computational time.

Critical value of electron velocity, separating electrons into fast and slow subgroups, can be obtained from the Courant condition, $v_{\rm e,\,crit} \leq \Delta x/(\Delta t\, S_{\rm se})$. Additional restrictions imposed on the time step Δt

$$P_{\rm se} = 1-\exp(-\nu_{\rm e_{max}}\,(S_{\rm se}\Delta t)) << 1, \quad (10)$$

$$P_{\rm i} = 1-\exp(-\nu_{\rm i_{max}}\,(S_{\rm i}\Delta t)) << 1 \quad (11)$$

are required to keep collision probabilities of slow electrons and ions reasonably small [13]. Here $\nu_{e_{\rm max}}$ and $\nu_{i_{\rm max}}$ denote maximum values of total collision frequencies for electrons and ions respectively.

Slow electrons in sheath regions of discharge (including electrons emitted from the electrodes) may gain high velocities, thus violate the Courant condition before being transferred into the fast electron group. Therefore, in order to ensure reliable numerical results, all the sheath electrons are treated as fast ones and never subcycled.

3 Validation of the code

The conditions of the benchmark case II in Ref. [8] are employed to validate the performance of parallel 1d3v PIC/MCC code. Plasma of capacitive RF discharge in helium of density $32.1\times10^{20}\,{\rm m}^{-3}$ and temperature 300 K with parallel electrode configuration of amplitude 250 V and frequency 13.56 MHz is considered. Separation between the electrodes is 6.7 cm. (More details about the input and solution parameters can be found in the specified reference.) Code is implemented in fortran 90 and carried out using a computer with Intel Core $i7$ CPU. Comparison of the reference and the recent study results is given in Figure 4. Maximum relative error for the ion density profiles is found to be about 0.0165, which is quite satisfying for particle simulations.

4 The effect of number of super particles used in the PIC/MCC simulations

Kim et al. [16] mentioned importance of the effect of super particle weighting in PIC/MCC simulations on particle densities and mean electron temperature in the bulk plasma. Donkó et al. [2] investigated this effect in the case of DC (direct current) glow discharges. Turner [17] further extended these studies by also including Coulomb collisions into the models, at various pressures.

We consider a capacitively coupled RF discharge, driven by a sinusoidal voltage source, with $V = 250\,\mathrm{V}$, at frequency $f = 13.56\,\mathrm{MHz}$. Distance between the electrodes is $L = 2.5\,\mathrm{cm}$. The left electrode is grounded, $\varphi|_{x=0} = 0$, the right electrode voltage varies according to $\varphi|_{x=L} = V\cos(2\pi f t)$, where t is the simulation time.

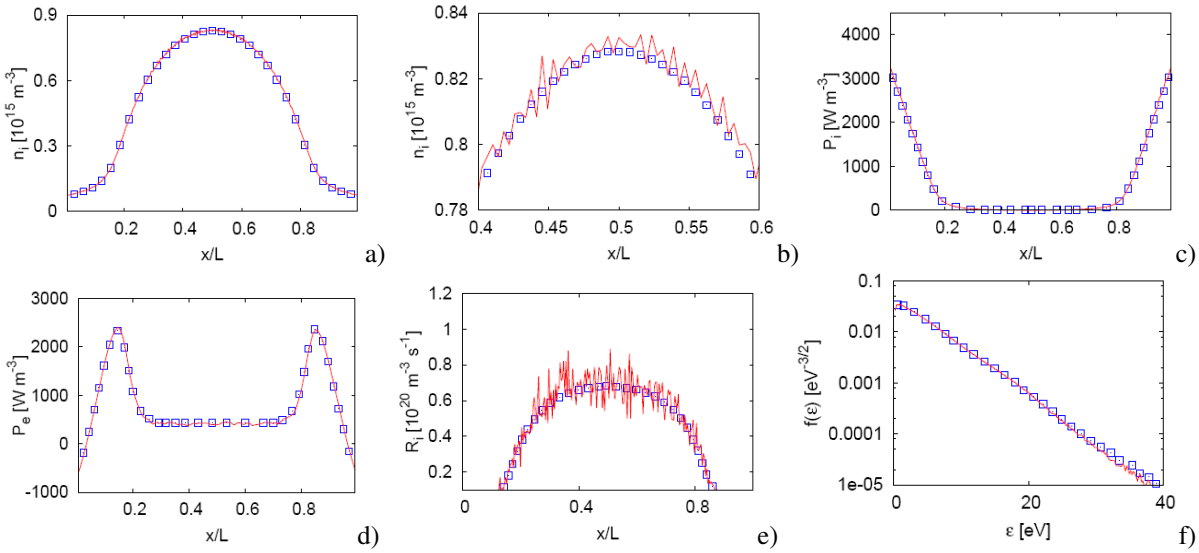

Fig. 4 The box symbols refer to the case II in Ref. [8], and continuous lines to recent study. (a) Ion density profile, (b) ion density profile at the center of the discharge, (c) ion heating rate, (d) electron heating rate, (e) ionization source, (f) normalized electron energy distribution function $f(\varepsilon)$.

Background gas is pure argon at temperature 350 K and pressure 10 Pa. Secondary electron emission coefficient is 0.1. Using 600 grid points, we have done 6 different simulations by only changing the super particle weightings. Simulations are carried out using HPC resources [18]. The information about the simulations is given in Table 1.

Table 1 Effect of particle weighting on the total number of super electrons, average number of super electrons per grid cell, Debye length, λ_D, and number of super electrons per Debye length, N_D, at the end of the simulations, $t \approx 7.37 \times 10^{-5}$ s. (λ_D and N_D are calculated at the midplane of the discharge.)

Simulation No	Weighting	Total number of super electrons	Average number of super electrons per grid cell	Debye length λ_D (m)	N_D
1	41.7×10^8	15746	26	1.74×10^{-4}	231
2	20.8×10^8	33822	56	1.56×10^{-4}	455
3	5.2×10^8	173054	288	1.11×10^{-4}	1713
4	3.0×10^8	339532	566	9.54×10^{-5}	2917
5	2.0×10^8	537500	896	8.79×10^{-5}	4272
6	1.5×10^8	737316	1229	8.42×10^{-5}	5635

Results presented in Figures 5–8 (as well as in Table 1) correspond to the simulation time $t \approx 7.37 \times 10^{-5}$ s (which covers 2×10^7 iterations and about 1100 simulation cycles), achieving converged solutions. Charged particle densities increase with the increasing number of super particles (see Figure 5). As expected, numerical noise is reduced significantly. The increase in the density tends to saturate, and a converged profile is achieved, as seen in Figure 5d. Using about 1200 super electrons per grid cells, weighting independent results are achieved for the density profiles. The parameter N_D listed in Table 1 corresponds to maximum number of super particles per Debye length evaluated at the discharge midplane where the concentration of the particles is the highest.

Figure 6 shows profiles of total current density $J_\mathrm{t} = J_\mathrm{e} + J_\mathrm{i} + J_\mathrm{d}$ obtained from simulations #1 and #6 at three different times within the RF period ($\omega t/2\pi = 0.25$, $\omega t/2\pi = 0.50$, $\omega t/2\pi = 0.75$). Electron and ion current

densities $J_{\rm e}$ and $J_{\rm i}$ and displacement current density $J_{\rm d}$ at grid point k are determined from

$$J_{{\rm e}_k} = n_{{\rm e}_k} < v_{{\rm e}x} > q_{\rm e}, \quad (12)$$

$$J_{{\rm i}_k} = n_{{\rm i}_k} < v_{{\rm i}x} > q_{\rm i}, \quad (13)$$

$$J_{{\rm d}_k} = \varepsilon_0 \frac{\partial E_k}{\partial t}, \quad (14)$$

where $< v_{{\rm e}x} >$ and $< v_{{\rm i}x} >$ denote x components of mean electron and ion velocities at point k. Higher noise and noticeable total current discontinuity is remarkable for the simulations using less number of super particles. However, mean values of the corresponding total current densities are close to each other. Also, it should be noted that constant profile of total current density as a function of position supports the validity of the simulation (Fig. 6b).

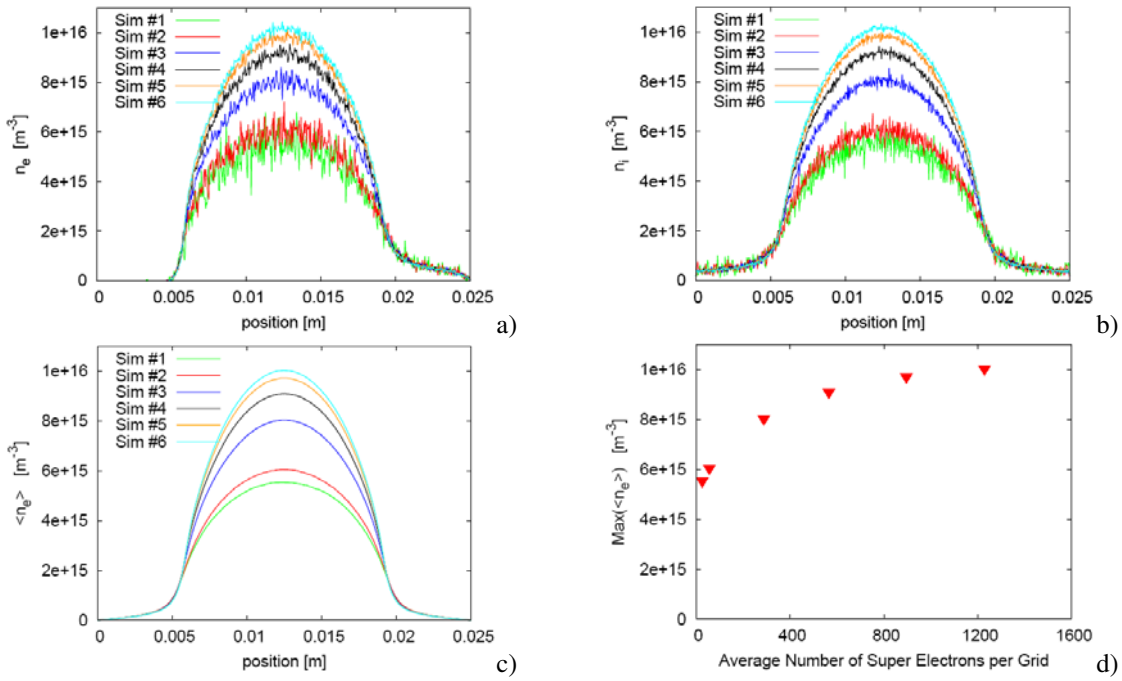

Fig. 5 Effect of the super particle weightings on (a) the electron density profiles, (b) the ion density profiles, (c) the mean electron density profile over one RF cycle, (d) the maximum electron density vs average number of super electrons per grid, at simulation time $t \approx 7.37 \times 10^{-5}$ s.

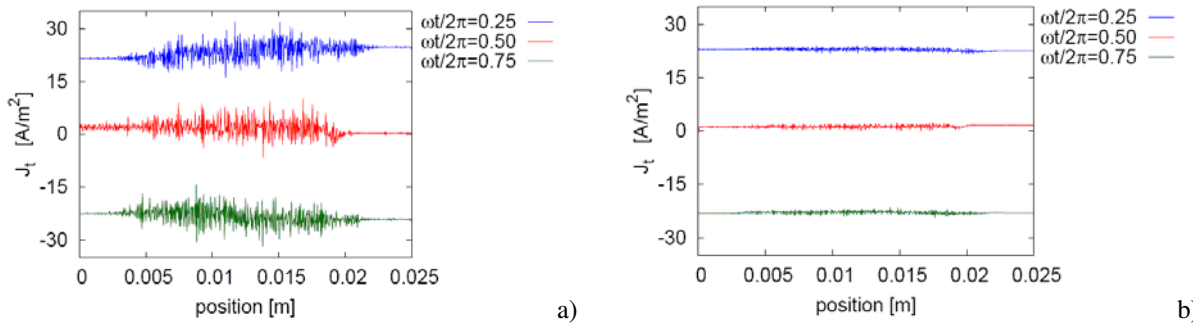

Fig. 6 Effect of the super particle weightings on (a) Total current density profile for simulation #1, (b) Total current density profile for simulation #6 at time $\omega t/2\pi = 0.25$, $\omega t/2\pi = 0.50$, and $\omega t/2\pi = 0.75$.

Another marked difference is that the averaged electric field profiles tend to become less inclined and noisy at the center of the discharge with more particles involved in simulations (Figure 7 (a, b)).

Mean energy profiles of both ions and electrons in the quasi-neutral region (center of the discharge) are highly dependent on the particle weighting: more particles used, lesser the average energies (Figure 7 (c, d)).

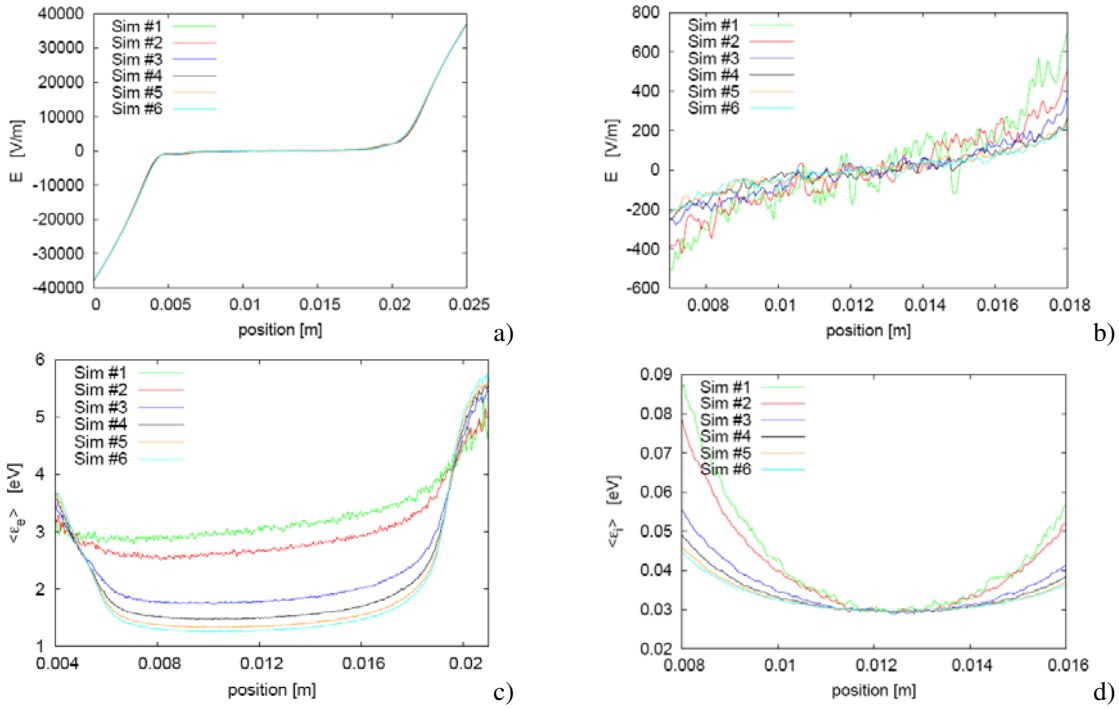

Fig. 7 Effect of the super particle weighting on (a) electric field profiles, (b) electric field profile details at the center of the discharge, (c) mean electron energy profiles at the center of the discharge, (d) mean ion energy profiles at the center of the discharge. Time $\omega t/2\pi = 0.25$ of the RF period.

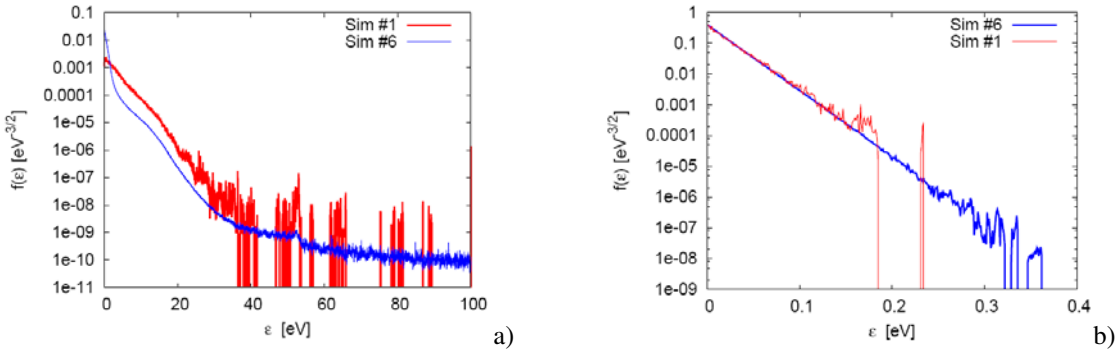

Fig. 8 Effect of the super particle weighting on (a) electron energy distribution function at the center of the discharge, (b) ion energy distribution function at the center of the discharge. Time $\omega t/2\pi = 0.25$ of the RF period.

Finally, as can be seen from Figure 8, ion energy distribution functions (edf) retains the Maxwellian shape independent on the weighting used in the simulations. But for the electrons, if the particle weighting is not adequate, edf becomes distorted, hence the simulations could not predict the distribution function correctly (Figure 8 (a)). Here the energy distribution functions are normalized according with

$$\int_0^\infty \sqrt{\varepsilon}\, f(\varepsilon)\, d\varepsilon = 1. \tag{15}$$

5 Conclusions

A parallel Particle in Cell/Monte Carlo Collision (PIC/MCC) fortran code for glow discharge simulations is developed and verified. The method is based on the simultaneous solutions of the Lorentz equations of motion of super particles, coupled with the Poisson's equation for electric field. Collisions between the particles are modelled by the Monte Carlo method.

The effect of particle weighting on the PIC simulation results has been studied. This issue is often ignored in particle studies, even though it can play a crucial role in developing an efficient particle simulation algorithm.

In the case of capacitive RF discharge in argon gas, effects of particle weighting on the discharge characteristics, such as charged particle densities, electric field and current density, average energies of charged particles, and energy distribution functions, are demonstrated. Results show that the discharge characteristics are highly dependent on the number of particles used in simulations. To obtain weighting independent results in the studied parameter regime, about 1200 super particles per grid cell are needed. Corresponding number of super particles per Debye length, N_{D}, at the discharge midplane is about 5600.

Acknowledgements The help of Z. Donkó and M. Turner during the refinement and validation of the codes is gratefully acknowledged. The authors would also like to thank E. Eylenceoğlu for his contribution with valuable discussions. The HPC resources were provided by the Department of Computer Engineering at METU. This work was supported by the research grant 210T072 from the Scientic and Technical Research Council of Turkey (TUBITAK).

References

[1] A. Bogaerts, E. Neyts, R. Gijbels, and J. Mullen, Spectrochim. Acta B **57**, 609 (2002).
[2] Z. Donkó, P. Hartmann, and K. Kutasi, Plasma Sources Sci. Technol. **15**, 178 (2006).
[3] I. Rafatov, E.A. Bogdanov, and A.A. Kudryavtsev, Phys. Plasmas **19**, 033502 (2012).
[4] E.A. Bogdanov, S.F. Adams, V.I. Demidov, A.A. Kudryavtsev, and J. M. Williamson, Phys. Plasmas **17**, 103502 (2010).
[5] L.D. Tsendin, Physics-Uspekhi **53**, 133 (2010).
[6] A. Derzsi, P. Hartmann, I. Korolov I, J. Karácsony, G. Bono, and Z. Donkó, J. Physc. D: Appl. Physc. **42**, 225204 (2009).
[7] Z. Donkó, Plasma Sources Sci. Technol. **20**, 024001 (2011).
[8] M.M. Turner, A. Derzsi, Z. Donkó, D. Eremin, and S.J. Kelly, Phys. Plasmas **20**, 013507 (2013).
[9] S. Ross, A First Course in Probability (Pearson, New Jersey, 2010), p. 278.
[10] C. K. Birdsall, IEEE Trans. Plasma Sci. **19**, 65 (1991).
[11] Q. Wang, J. Economou, and V.M. Donnelly, J. Appl. Phys. **100**, 023301 (2006).
[12] A.V. Phelps, J. Appl. Phys. **76**, 747 (1994).
[13] J.P. Verboncoeur, Plasma Phys. Control. Fusion **47**, A231 (2005).
[14] V. Vahedi and M. Surrendra, Computer Physics Communications **87**, 179 (1995).
[15] E. Kawamura, C.K. Birdsall, and V. Vahedi, Plasma Sources Sci. Technol. **9**, 413 (2000).
[16] H.C. Kim, F. Iza, S.S. Yang , M. Radmilović-Radjenović, and J. K. Lee, J. Phys. D: Appl. Phys. **38**, 283 (2005).
[17] M.M. Turner, Phys. Plasmas **13**, 033506 (2006).
[18] HPC Facility of the Department of Computer Engineering at METU (http://www.ceng.metu.edu.tr/hpc/index)

